UC Irvine
Faculty Publications

Title

Change in net primary production and heterotrophic respiration: How much is necessary to sustain the terrestrial carbon sink?

Permalink

Journal

ISSN

Authors

Thompson, Matthew V
Randerson, James T
Malmstrom, Carolyn M
et al.

Publication Date

DOI

Copyright Information

Peer reviewed

Change in net primary production and heterotrophic respiration: How much is necessary to sustain the terrestrial carbon sink?

Matthew V. Thompson,[1,2] James T. Randerson,[1] Carolyn M. Malmström,[1] and Christopher B. Field

Department of Plant Biology, Carnegie Institution of Washington, Stanford, California

Abstract. In recent years, the chief approaches used to describe the terrestrial carbon sink have been either (1) inferential, based on changes in the carbon content of the atmosphere and other elements of the global carbon cycle, or (2) mechanistic, applying our knowledge of terrestrial ecology to ecosystem scale processes. In this study, the two approaches are integrated by determining the change in terrestrial properties necessary to match inferred change in terrestrial carbon storage. In addition, a useful mathematical framework is developed for understanding the important features of the terrestrial carbon sink. The Carnegie-Ames-Stanford Approach (CASA) biosphere model, a terrestrial carbon cycle model that uses a calibrated, semimechanistic net primary production model and a mechanistic plant and soil carbon turnover model, is employed to explore carbon turnover dynamics in terms of the specific features of terrestrial ecosystems that are most important for the potential development of a carbon sink and to determine the variation in net primary production (NPP) necessary to satisfy various carbon sink estimates. Given the existence of a stimulatory mechanism acting on terrestrial NPP, net ecosystem uptake is expected to be largest where NPP is high and the turnover of carbon through plants and the soil is slow. In addition, it was found that (1) long-term, climate-induced change in heterotrophic respiration is not as important in determining long-term carbon exchange as is change in NPP and (2) the terrestrial carbon sink rate is determined not by the cumulative increase in production over some pre-industrial baseline, but rather by the rate of increase in production over the industrial period.

Introduction

Currently, balancing the global carbon budget requires a net flux of carbon out of the atmosphere and into the terrestrial biosphere of the order of 1 to 2 Gt C yr^{-1} (1 Gt = 10^{12} kg) [*Enting and Mansbridge*, 1991; *Moore and Braswell*, 1994; *Sarmiento et al.*, 1995; *Schimel et al.*, 1995; *Tans et al.*, 1990]. The difficulty with this flux is that it has never been observed directly. To do so would require long-term monitoring of carbon storage in the terrestrial biosphere, which is difficult for a number of reasons: (1) the estimated size of the sink (1-2 Gt C yr^{-1}) is almost 2 orders of magnitude smaller than the total amount of carbon that flows through the terrestrial biosphere each year [*Fung et al.*, 1983; *Lieth*, 1975; *Maisongrande et al.*, 1995; *Melillo et al.*, 1993; *Potter et al.*, 1993] and almost 3 orders of magnitude smaller than the amount of carbon stored [*Post et al.*, 1982], begging the question of whether our sensitivity to carbon storage in plants and soils is great enough to resolve any change; (2) high natural spatial heterogeneity of carbon storage requires comprehensive measurement of relatively large regions; and (3) strong temporal and spatial variability in events such as fire, human disturbance, and secondary succession demands sophisticated scaling methods.

The magnitude of the terrestrial carbon sink is generally best resolved indirectly by calculating the difference between the growth rate of atmospheric CO_2 [*Conway et al.*, 1994] and the sum of land use change [*Houghton*, 1995], fossil fuel combustion [*Marland and Rotty*, 1984], and oceanic exchange [*Siegenthaler and Sarmiento*, 1993]. Some information about the spatial distribution of the carbon sink can be obtained by deconvolving the seasonal and spatial variation in atmospheric $^{12}CO_2$ and $^{13}CO_2$ using atmospheric tracer-transport models [*Ciais et al.*, 1995; *Enting*, 1995]. Direct methods have been adopted in recent years using eddy covariance techniques to measure regional carbon exchange [*Grace et al.*, 1995] and extrapolating these measurements to larger scales, but questions regarding the applicability of individual, isolated measurements to the regional or global scale prevent such data from providing a complete picture.

Although all of the above approaches provide a wealth of useful information, as well as some constraint on the size and location of the sink, none of them provide both direct and comprehensive accounting of changes in the size and location of terrestrial carbon storage and as such do not provide a clear definition of the global location or magnitude of the missing sink; it is unlikely that any such delineation is immediately

---

[1] Also at Department of Biological Sciences, Stanford University, Stanford, California.

[2] Now at Department of Organismic and Evolutionary Biology, Harvard University, Cambridge, Massachusetts.

forthcoming. As a result, other approaches are necessary. To fill the vacuum, carbon cycle models have become more common as heuristic tools for understanding carbon exchange [Houghton, 1987; Moore and Braswell, 1994; Parton et al., 1995]. A direct, synthetic model approach allows terrestrial carbon flux to be defined in terms of the processes that control it: production and respiration. The size and nature of the sink, as well as any constraints on its location, can then be roughly characterized with the use of these models which take advantage of our knowledge of the behavior of the terrestrial biosphere [Friedlingstein et al., 1995]. Many researchers have estimated the size and location of the sink in this way [Gifford, 1994; Hudson et al., 1994; Schindler and Bayley, 1993].

We take the next step by combining the inferential approaches mentioned above with the mechanistic approach, calculating the variation in different carbon fluxes necessary to satisfy an inferred estimate of the sink. In this study, we use the Carnegie-Ames-Stanford Approach (CASA) biosphere model [Field et al., 1995; Potter et al., 1993] to model changes in production and respiration through time and space. The CASA carbon turnover model mechanistically constrains the flow of carbon out of the terrestrial biosphere through heterotrophic respiration (R_h) which is dependent primarily on inputs of new carbon and changes in climate. Thus net global carbon balance in CASA depends primarily on variation in net primary production (NPP) and historical climate variation and its effects on R_h.

We estimate the change in NPP that is necessary through time to satisfy changes in the global carbon cycle. We do not focus on any single stimulation mechanism, such as changes in climate, CO_2, or nitrogen fertilization, as in the work of Friedlingstein et al. [1995]. Instead, we select the NPP stimulation that under the model produces exactly the estimated sink. In this paper, we develop this in two directions: first, we explore the dynamics of carbon exchange under increasing NPP and how changes in climate affect the link between NPP and the sink; and second, we calculate the variation in NPP necessary to satisfy several estimates of the terrestrial carbon sink globally and when forced into specific geographical regions.

Model Approach

Net carbon exchange in terrestrial ecosystems is controlled by a number of different processes, including primary production, autotrophic and heterotrophic respiration, land use change, fires and forest regrowth [Houghton, 1995], and dissolved organic and inorganic carbon flow in river systems [Vorosmarty et al., 1989]. In this study, following Friedlingstein et al. [1995], we simplify the budget to include only net primary production and heterotrophic respiration:

$$\frac{dC(t)}{dt} = P(t) - R_h(C, climate) \tag{1}$$

where $C(t)$ represents terrestrial carbon storage and $P(t)$ represents net primary production, both functions of time. The term $dC(t)/dt$ is the annual increment in carbon storage or net ecosystem production.

By (1), if $dC(t)/dt$ is prescribed and R_h depends on C and climate, we can estimate the course of P over time. Conversely, if R_h is constrained through changes in carbon

storage due to past changes in P, we should then be able to determine the size of the sink by changing $P(t)$. If P increases at a constant annual rate, thus increasing the size of the carbon pools in the system, then R_h will also increase (since respiration is a supply-based process) but with a time lag such that changes in R_h will always trail changes in P [Friedlingstein et al., 1995]. Eventually, the relative rate of increase in R_h will nearly equal that of P and a constant, nonzero sink will form, the magnitude of which in this special case will depend on the relative rate of increase in P and the turnover time of carbon. This is best illustrated in a simple model.

First, assume that P is a linear function of time, such that

$$P(t) = P_o\left[rt + 1\right], \tag{2}$$

where P_o is the magnitude of P before the increase begins and r is the relative rate of increase in P such that

$$r = \frac{1}{P_o}\frac{dP}{dt}. \tag{3}$$

Also, assume that heterotrophic respiration is linearly dependent on the carbon stored in the system,

$$R_h(C) = kC, \tag{4}$$

where k is the first-order, climate dependent rate constant for decomposition of a single terrestrial carbon pool C. We can calculate the sink through time by inserting (2) and (4) into (1) to get

$$\frac{dC(t)}{dt} = P_o\left[rt + 1\right] - kC(t). \tag{5}$$

Solving for $C(t)$, we find that

$$C(t) = \frac{P_o}{k}\left[rt + 1\right] - \frac{P_o r}{k^2}\left[1 - e^{-kt}\right], \tag{6}$$

and that differentiating both sides gives

$$\frac{dC(t)}{dt} = \frac{P_o r}{k}\left[1 - e^{-kt}\right]. \tag{7}$$

A simple solution for (7) exists when $t \to \infty$. If we let

$$\tau = \frac{1}{k}, \tag{8}$$

where τ is the turnover time of carbon in the ecosystem, and allow t to become very large, carbon exchange approaches a stable value that is proportional to P_o, r, and τ:

$$\frac{dC}{dt} = P_o\, r\, \tau\bigg|_{t \to \infty}. \tag{9}$$

Thus the size of a stable sink after a long period of increase in NPP is directly proportional to initial NPP, the relative rate of increase in NPP, and the the turnover time of carbon in the system.

The sink calculated by (9) is reached asymptotically as $t \to \infty$, as seen in (7). The time t required for the sink to reach a fraction f of the sink in (9) can be found by setting the right side of (7) equal to f times the right side of (9) to get

$$t = -\tau \ln(1 - f). \tag{10}$$
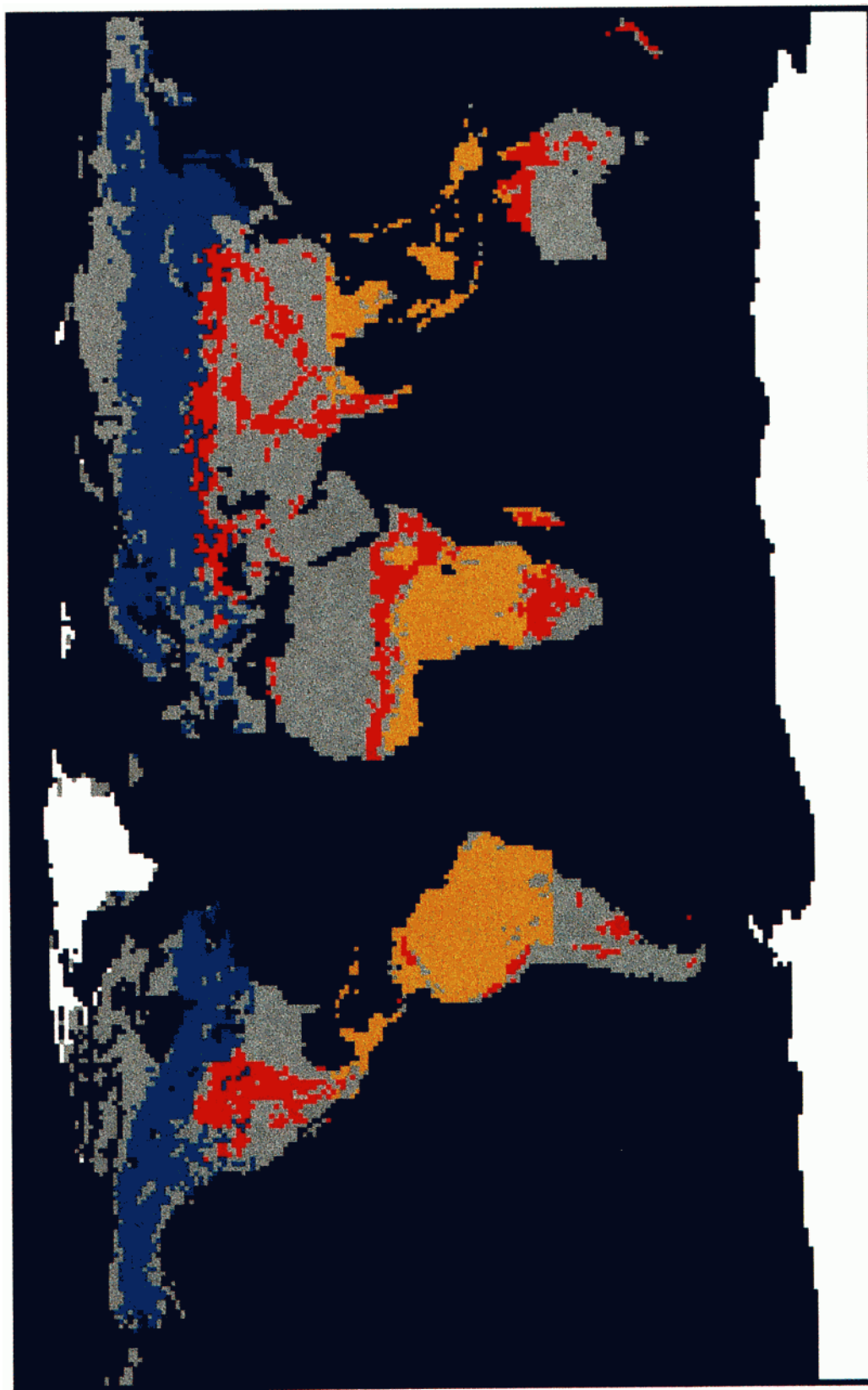
Plate 1. Geographical regions in experiment 3 into which we force the Ho sink. Blue (zone 1) represents all of vegetation classes 3, 4, and 5 (Table 1) north of 45° N. Red (zone 2) represents all preagricultural and postagricultural grassland cells. Yellow (zone 3) represents all of vegetation classes 1 and 6 (Table 1) between 23° N and 23° S. Gray (zone 4) represents all other ice-free land area. White represents ice.

For example, it would take 46 years for an ecosystem with a carbon residence time of 20 years to reach 90% (or $f = 0.9$) of the sink estimated in (9), 92 years to reach 99% of the sink, and 138 years to reach 99.9% of the sink.

If we extend (9) to the entire terrestrial biosphere and assume a global carbon turnover time of 20 years, an initial global NPP of 50 Gt C and a relative rate of increase in NPP of 0.2% yr^{-1}, a stable sink of the order of 2 Gt C yr^{-1} forms, reaching 90% of its final size in under 50 years. In other words, a 0.1 Gt annual increase in global NPP is sufficient to create and sustain a 1.8 Gt annual carbon sink within the post–World War II era.

We extend the simple model in (1)-(10) to the more complex case of CASA, allowing us to consider multicomponent biomass and soil organic matter pools. We are then able to manipulate the annual magnitude of NPP to create carbon sources and sinks in different regions, through time with some realism. Given an historical estimate of the magnitude of the sink over time, we can estimate for every year the carbon sink has been estimated the change in NPP necessary to sustain that sink.

Model Description

We use CASA v1.2, based on CASA v1.0 [Potter et al., 1993] and CASA v1.1 [Field et al., 1995], which has been revised to include a new soil model developed by Parton et al. [1993], an improvement to the litterfall and heterotrophic respiration algorithm [Randerson et al., 1996], and the addition of biomass pools with turnover times set by Kohlmaier et al. [in press]. CASA calculates NPP on a monthly time scale as the product of intercepted photosynthetically active radiation (IPAR) and light use efficiency ε [Field et al., 1995; Potter et al., 1993]:

$$P(x,t) = IPAR(x,t) \; \varepsilon(x,t) . \tag{11}$$

IPAR is the product of the fraction of photosynthetically active radiation intercepted by the canopy (FPAR), the surface solar irradiance S, and a factor 0.5 which represents the fraction of surface solar irradiance that is photosynthetically active,

$$IPAR(x,t) = 0.5 \; FPAR(x,t) \; S(x,t) , \tag{12}$$

while light use efficiency is the product of a globally uniform maximum light use efficiency, ε^*, one water stress scalar, and two temperature stress scalars that vary locally:

$$\varepsilon(x,t) = W_\varepsilon(x,t) \; T_{\varepsilon 1}(x,t) \; T_{\varepsilon 2}(x,t) \; \varepsilon^* . \tag{13}$$

CASA uses monthly inputs of normalized difference vegetation index (NDVI) to calculate FPAR and monthly temperature and precipitation to calculate the stress scalars. The value ε^* is calculated from a least squares fit of annual NPP values calculated by CASA against observed values for sites corresponding to various grid cells [Field et al., 1995; Potter et al., 1993]. The calibrated value for ε^* used in this study was 0.489 g C MJ^{-1} PAR, based on global NPP derived for experiments 1, 2, and 3 (described below).

The flow of carbon from the atmosphere to live plant biomass and to the soil through litterfall is described in Figure 1. NPP is allocated to wood, leaves and roots at a 1:1:1 ratio,

except in grasslands, tundra, and agriculture where there is no modeled wood and the ratio of leaves to roots is 1:1. CASA sets live biomass turnover times for leaves (τ_L), roots (τ_R), and wood (τ_W) by vegetation type derived from the work of Kohlmaier et al. [in press] (Table 1). Leaf, root, and coarse woody litter exits the live biomass pools at an annual rate proportional to the amount of biomass present and inversely proportional to the turnover time (year). The seasonal distribution of leaf litterfall is determined from seasonal changes in leaf area index (LAI) calculated from NDVI data. Seasonal root mortality is also proportional to changes in LAI but takes into account changes in leaf production to better distribute the timing of root activity. Coarse woody debris production is assumed constant year-round [Randerson et al., 1996].

Soil carbon pools are divided into three broad categories: litter, microbial and soil organic matter pools. Litter pools are subdivided into structural and metabolic pools, and the structural litter pools are further subdivided into lignin and cellulose fractions, which flow into the slow and microbial pools, respectively. The split of leaf and root litter into metabolic and structural litter is determined by the lignin:N ratio of the entering litter, which is a function of vegetation type (Table 1). The split between the two structural fractions is determined by the lignin content of the litter. All carbon flows are mediated by temperature and water scalars and by soil texture as in the work of Parton et al. [1993]. Respiration from each pool is proportional to the flow of carbon from each pool times a fraction equal to $(1 - M_\varepsilon)$, where M_ε is the microbial assimilation efficiency of each pool:

$$R_i = (1 - M_{\varepsilon,i}) \; T_S \; W_S \; k_i \; C_i , \tag{14}$$

where R_i is the rate of respiration from soil pool i, T_S and W_S are temperature and water scalars, respectively, and k_i is the rate constant for pool i under optimal conditions.

The temperature scalar T_S is calculated from a Q_{10} equation,

$$T_S = Q_{10}^{(T_{AIR} - 30)/10} , \tag{15}$$

where T_{AIR} is in degrees centigrade and T_S is a scalar which approaches 0 as $T_{AIR} \rightarrow -\infty$ and equals 1 when T_{AIR} equals 30°C. We choose $Q_{10} = 1.5$ for this study [Heimann et al., 1989; Holland et al., 1995]. A Q_{10} of 2.0 to 2.4 may be more realistic for modeling a direct response of soil microbes to surrounding soil temperature, and it is in all probability better to use an entirely different temperature function altogether [Lloyd and Taylor, 1994], but at this time, it appears that a Q_{10} equation with a Q_{10} value of 1.5 is most appropriate when using monthly air temperature as a surrogate for soil temperature [Raich and Potter, 1995], as we do. It should be noted that changing Q_{10} does more than affect the seasonality of heterotrophic respiration. It also changes the rate of respiration, which in turn affects carbon storage and its rate of turnover. A full definition of W_S and the soil moisture model can be found in the work of Randerson et al. [1996] and Potter et al. [1993].

Input Data

Global data sets. We used a compilation of multiyear global data sets to calculate mean NPP and soil moisture for a single year. This compilation contains monthly Fourier-adjusted, solar zenith angle corrected, interpolated and recon-
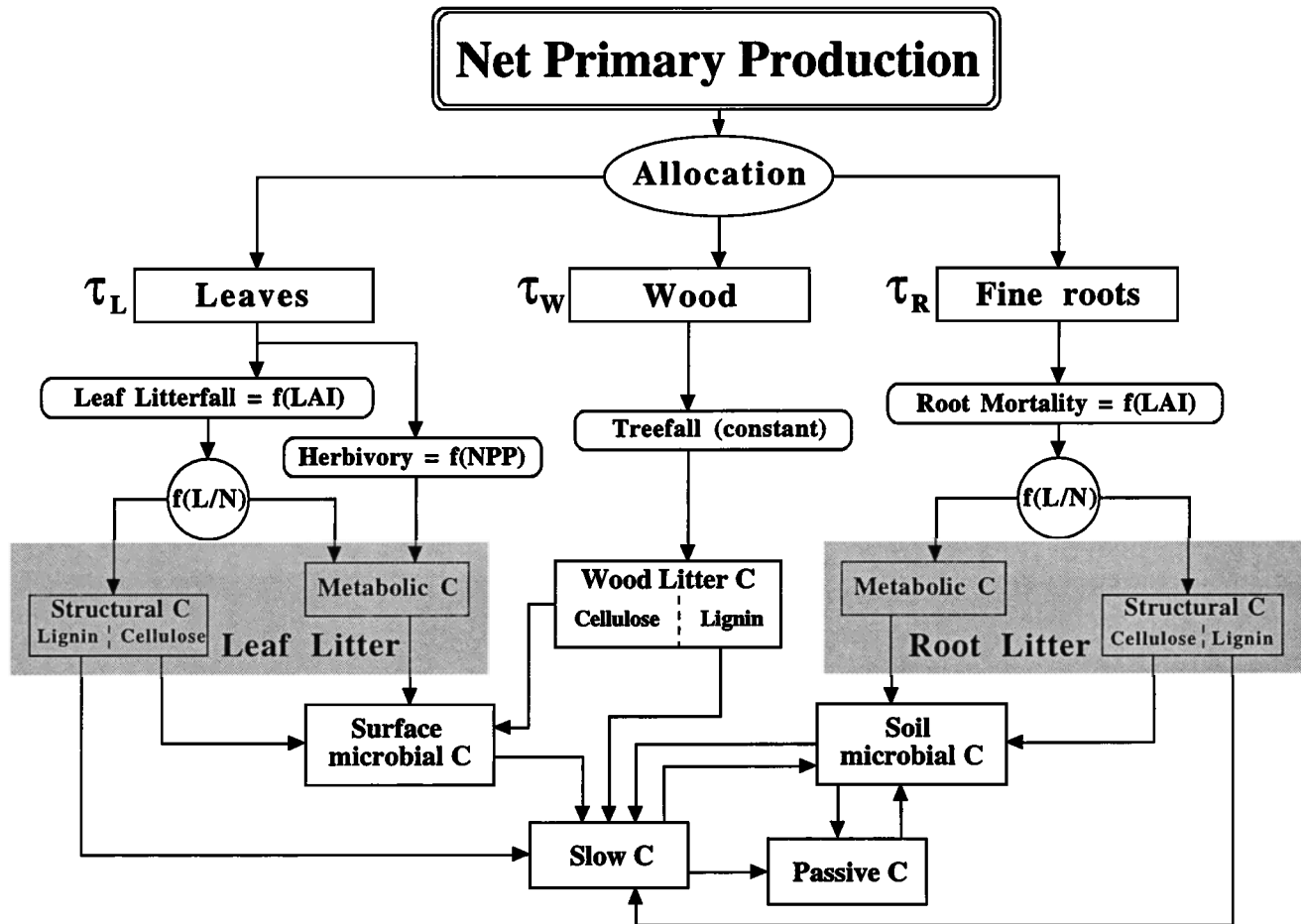
Figure 1. The flow of carbon through live biomass, litter, and soil organic matter pools as described by the Carnegie-Ames-Stanford Approach (CASA) biosphere model.

structed (FASIR) advanced very high resolution radiometer (AVHRR) NDVI data as well as Fourier-adjusted, solar zenith angle corrected (FAS) AVHRR NDVI data [Los et al., 1994; Sellers et al., 1994] for 1990, used for calculating FPAR and LAI, respectively. The compilation also contains mean monthly precipitation and air temperature data [Shea, 1986]

for the period from 1950 to 1979, as well as monthly surface solar irradiance [Bishop and Rossow, 1991] for 1990. To delineate different vegetation classes, we used the NDVI-derived vegetation classification of Defries and Townshend [1994], which consists of 12 classes, including ice, agriculture, and deserts. Soil texture was defined according to Zobler [1986] in

Table 1. Vegetation Parameters Used in the CASA Biosphere Model, by Vegetation Class, as Defined by *Defries and Townshend* [1994]

Vegetation Class	Land Area %	C:N	Lignin %	τ_W, year	τ_L, τ_R, year	Deviation %
Broadleaf evergreen trees	10.1	40	20	41.0	1.8	89.7
Broadleaf deciduous trees	2.5	50	20	58.0	1.2	94.8
Mixed broadleaf and needleleaf trees	5.0	65	22	58.0	1.2	92.8
Needleleaf evergreen trees	9.8	80	25	42.0	5.0	91.9
Needleleaf deciduous trees	4.3	50	20	27.0	1.8	90.8
Broadleaf trees with ground cover	16.4	50	15	25.0	1.8	91.5
Perennial grassland	6.8	50	10	0.0	1.5	87.2
Broadleaf shrubs	8.3	65	20	5.5	1.0	95.2
Tundra	5.3	50	15	0.0	2.8	83.1
Hot and cold desert	12.7	50	15	1.0	1.0	94.6
Agriculture	18.7	40	10	0.0	1.0	81.9

The values τ_W, τ_L, and τ_R are the turnover times for wood, leaves, and fine roots, respectively, from *Kohlmaier et al.* [in press]. Included is the percent deviation of the carbon sink calculated iteratively with CASA, from the sink calculated analytically from (9). See text for explanation.
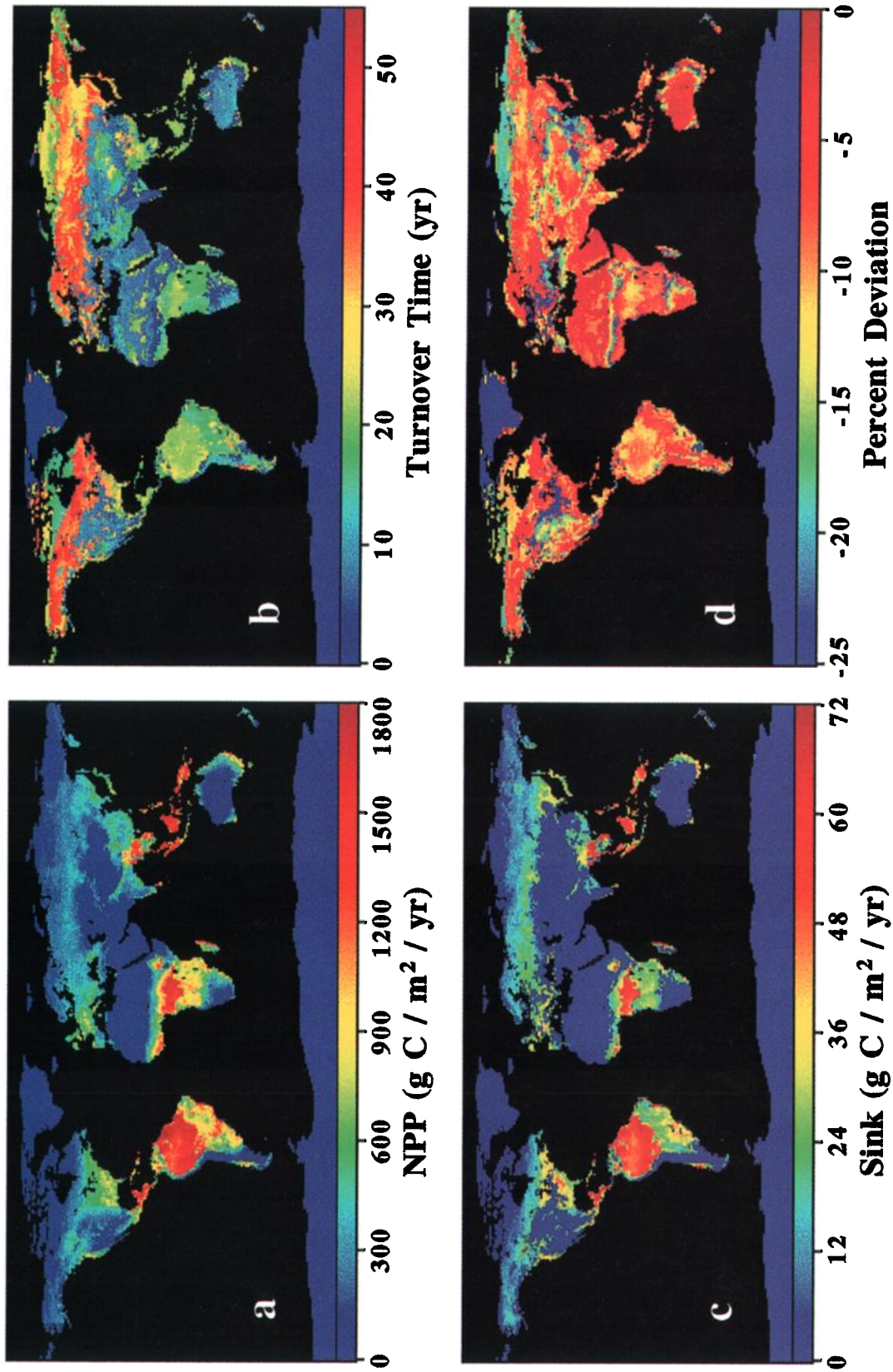
Plate 2. Constant rate of increase in global NPP. (a) The distribution of annual NPP derived from the standard mean input data sets (global NPP = 57.8 Gt C, see Initial Condition section under Model Experiments). (b) The mean residence time of carbon at each pixel defined as total carbon storage in both plants and soil divided by annual NPP (global area weighted average τ = 17.9 years). (c) The annual carbon sink at each pixel after 500 years of 0.2% yr^{-1} increase in annual NPP (global sink = 2.04 Gt C yr^{-1}). (d) The deviation of the carbon sink in Plate 2c from the sink calculated in (9) (2.25 Gt C yr^{-1}).

Table 2. Soil Parameters Used in the CASA Biosphere Model, by Soil Texture Class, as Defined by *Zobler* [1986]

| Soil Texture Class	Clay Fraction	Silt Fraction	Sand Fraction	Deviation, %
Organic	0.20	0.20	0.20	90.1
Coarse	0.09	0.08	0.09	93.1
Coarse / medium	0.20	0.20	0.20	92.3
Medium	0.30	0.33	0.30	88.8
Fine / medium	0.48	0.25	0.48	87.3
Fine	0.67	0.67	0.67	86.4
Lithosol	0.20	0.20	0.20	89.2

Included is the percent deviation of the carbon sink calculated iteratively with CASA, from the sink calculated analytically from Equation (9). See text for explanation.

seven classes (Table 2), including a lithosol and an organic soil.

Climate anomalies. In addition to the mean monthly precipitation and surface temperature data, we used monthly air temperature and seasonal precipitation anomalies to constrain heterotrophic respiration for the period of this study (1880-1990). Monthly surface air temperature anomalies from 1880 through part of 1990 were obtained from a comprehensive anomaly data set [*Hansen and Lebedeff*, 1987; 1988] which has been updated continuously since 1987 and is available on-line. The data were provided spatially as described by *Hansen and Lebedeff* [1987], in the form of "boxes", "subboxes" and "zones"; we regridded the data to a 1°x1° matrix. Seasonal precipitation anomalies were derived from *Baker et al.* [1995], which is also available on-line. We used their data starting in 1880 regridded from a 4°x5° to a 1°x1° matrix.

Sink estimates. Two types of sink estimates were used in this study: (1) long-term source/sink estimates [*Houghton,* 1993; *Sarmiento et al.,* 1995] and (2) short-term source/sink estimates [*Francey et al.,* 1995; *Keeling et al.,* 1995]. The long-term estimates cover the period from 1766 to 1990 and are single deconvolutions of available atmospheric flux data [*Houghton,* 1993; *Sarmiento et al.,* 1995], calculated by subtracting an estimate of the carbon flux due to land use change, a modeled estimate of carbon exchange with the oceans, and estimates of fossil fuel emissions, from the growth rate of atmospheric CO_2. The *Houghton* [1993] (hereafter known as Ho) sink estimate is based on smoothed atmospheric CO_2 data obtained from trapped air bubbles in the Siple ice cores [*Friedli et al.,* 1986; *Neftel et al.,* 1982; *Siegenthaler et al.,* 1988], and from Mauna Loa after 1958 [*Keeling and Whorf,* 1994] (Figure 2). *Sarmiento et al.* [1995] (hereafter known as Sa) made a similar estimate but did not smooth the atmospheric data (Figure 2), as can be seen clearly in a comparison of the Sa deconvolution results with those of Ho (Figure 2). Variability in the Sa estimate declines considerably around 1958 when the Mauna Loa record begins, which is likely due to the increase in precision following the change in method. We use the Ho and Sa data for the period from 1880 to 1990, when the climatological data we require is available. Both estimate the cumulative carbon sink from 1880 to 1990 to have been near 93 Gt C (Table 3).

Two additional estimates of terrestrial carbon exchange were used, employing different methods than those of the long-term estimates and covering only the last 2 decades. The first estimate spans the period from 1977 to 1994 [*Keeling et al.,* 1995] (hereafter known as Ke), while the second spans the period from 1982 to 1992 [*Francey et al.,* 1995] (hereafter known as Fr). We used these data up to and including 1990. Both estimates perform a double deconvolution of measured
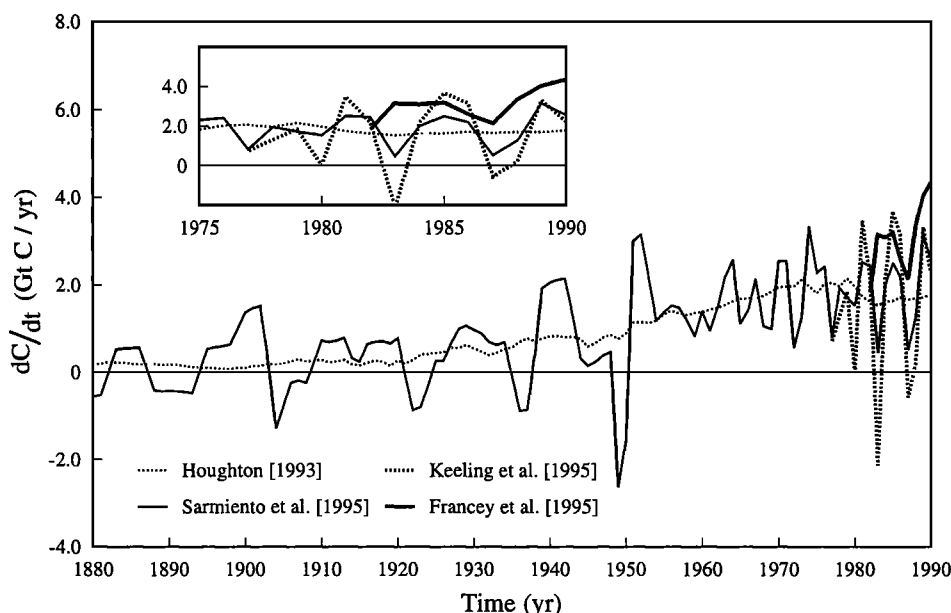
Figure 2. Long- and short-term sink estimates used in this study (see Table 3 for statistics). The sink estimates of Ho and Sa are overlaid with the sink estimates of Fr and Ke. The same data, from 1975 to 1990, is shown in the inset. The Fr and Ke sink estimates were additively adjusted by 1.6 Gt C yr^{-1} to subtract out carbon fluxes due to land use change (see text for explanation).

Table 3. Statistics for the Various Sink Estimates Used in This Study

Sink Estimate	Abbreviation	Period Covered	Cumulative Sink, Gt C	Annual Sink, 1977-1990 Gt C / yr
Houghton [1993]	Ho	1880-1990	92.5	1.8
Sarmiento et al. [1995]	Sa	1880-1990	93.4	1.8
Keeling et al. [1995]	Ke	1977-1990	21.6	1.5
Francey et al. [1995]	Fr	1982-1990	27.8	3.1[a]

Numbers presented for the short-term sink estimates, Fr and Ke, reflect the land use flux correction described in the text.
[a]Covers the period from 1982 to 1990, only.

^{12}C and ^{13}C. Ke employ continuous measurements of atmospheric CO_2 and measurements of δ^{13}C from both the Mauna Loa and South Pole monitoring stations. Fr use only data from Cape Grim, Tasmania. It should be noted that the Ke estimate is quantitatively similar to Sa but varies with a much larger amplitude (Figure 2). The similarity is likely due to the fact that both estimates use the same atmospheric data, and it suggests that the double deconvolution using δ^{13}C does not necessarily provide any discernibly new information.

There is some difficulty in comparing the long-term sink estimates with the short-term sink estimates. The short-term flux estimates account for all carbon exchange with the biosphere, and so do not distinguish between carbon fluxes due to land use change and fluxes due to the terrestrial sink, while the long-term estimates account only for the flux due to the sink. In order to make all four estimates comparable, it was necessary to modify the short-term estimates so that they no longer include the flux due to land use change. We did this by subtracting an estimated rate of flux due to land use change (~1.6 Gt C yr^{-1}, [*Houghton*, 1995]) from every year of both estimates. This is reflected in Figure 2. A key to the abbreviations for the different sink estimates used in this study, as well as some statistics on each, can be found in Table 3.

Model Experiments

All experiments performed in this study are listed briefly in Table 4.

Experiment 1. This experiment was performed to explore how the rate of carbon turnover affects the speed at which carbon sinks form under increasing NPP. Three cells were selected from the 1°x1° matrix used by the CASA model and were representative of a typical grassland site, a typical tropical forest site, and a typical boreal forest site. Each site was forced, from equilibrium, through a 0.2% yr^{-1} increase in NPP for 150 years, during which time the equilibrium climate was maintained.

Experiment 2. To assess the problem of experiment 1 globally, we forced every grid cell defined as ice-free land in the CASA model (Plate 1), from equilibrium, through a 500-year, 0.2% yr^{-1} increase in NPP, during which time the equilibrium climate and its effect on R_h were conserved. We chose the forcing time for this experiment by using (10). The largest steady-state residence time for any point is just over 70 years, so to come within 0.1% (f = 0.999, (10)) of the sink defined in (9), the points with the largest residence times required at least

500 years of forcing. The resulting sink for each point following the 500-year run was compared with results from (9).

Experiment 3. We then calculated carbon exchange for each cell but this time under variable climate and constant NPP from 1880 to 1990, using "1990" NPP (described below), in order to assess the sensitivity of the link between changes in NPP and the sink to changes in climate. Since the heterotrophic respiration term was the only calculated parameter in this experiment, we chose two different methods of calculating it. The first method employed a zero-order heterotrophic respiration model that used the temperature (T_S) and moisture (W_S) scalars on R_h [*Randerson et al.*, 1996], as noted in (14), to redistribute total NPP from 1880 to 1990 to heterotrophic respiration, seasonally and interannually [*Dai and Fung*, 1993; *Randerson et al.*, 1996]. Heterotrophic respiration for each month i, for each year j, and for each cell x was calculated as follows:

$$R_{h_{i,j,x}} = T_{S_{i,j,x}} \, W_{S_{i,j,x}} \, \frac{\sum\limits_{j=1880}^{1990} \sum\limits_{i=1}^{12} P_{i,j,x}}{\sum\limits_{j=1880}^{1990} \sum\limits_{i=1}^{12} T_{S_{i,j,x}} \, W_{S_{i,j,x}}} \qquad (16)$$

For the second run, CASA was employed. The resulting carbon exchange estimates calculated by the two models were compared against each other and against global temperature and precipitation anomalies.

Experiment 4. This experiment assumed the sink estimate of Ho as well as the precipitation and temperature anomalies described above [*Baker et al.*, 1995; *Hansen and Lebedeff*, 1987] to determine the NPP increase required to satisfy the entire historical sink estimate were it forced into one of the

Table 4. Experiments Performed in This Study

Experiment	Description
1	Carbon turnover dynamics for selected cells under invariant climate and linearly increasing NPP
2	Global carbon exchange under invariant climate and linearly increasing NPP
3	Global carbon exchange under constant NPP and variable climate
4	Regional forcing of NPP by historical sink estimate under variable climate
5	Global forcing of NPP by different historical sink estimates under variable climate

zones defined in Plate 1. A zone is defined as a set of all spatial cells falling within a specific geographical region. The sink was forced into each zone z by maintaining a uniform relative change in NPP within the zone, such that:

$$\frac{\partial r}{\partial x} = 0\bigg|_{t, x \in z} \qquad (17)$$

and a zero change in NPP everywhere else, such that:

$$\frac{\partial}{\partial t}\frac{\partial r}{\partial x} = 0\bigg|_{x \notin z} . \qquad (18)$$

Here x represents the spatial dimension and r is the same as in (3).

Four zones were examined: zone 1, zone 2, zone 3, and the combination of zones 1, 2, 3, and 4 (Plate 1). Heterotrophic respiration in all runs was allowed to vary in a first-order manner and in response to changes in climate. A linear β factor was calculated for each trajectory:

$$\beta = \frac{\left[P(t) - P_0\right]\big/ P_0}{\left[c(t) - c_0\right]\big/ c_0} \qquad (19)$$

where P_0 is net primary production in 1880, $P(t)$ is NPP in 1990, c_0 is the atmospheric concentration in parts per million by volume (ppmv) of CO_2 in 1880 (290 ppmv, [Neftel et al., 1994]), and $c(t)$ is the atmospheric concentration of CO_2 in 1990 (354 ppmv, [Keeling and Whorf, 1994]). This factor describes the trend in NPP expected were the entire sink due to CO_2 stimulation.

Experiment 5. This experiment found the change in global NPP necessary to satisfy different estimates of the global carbon sink over time, both historically and in recent decades, the same as in (17), but for the zone containing all ice-free land cells. Four runs were performed: the first deduced the variation in NPP necessary to meet the Ho sink estimate from 1880 to 1990; the second deduced the variation in NPP necessary to satisfy the Sa sink estimate from 1880 to 1990; the third run calculated the NPP variation from 1977 to 1990 required to satisfy the scaled Ke sink estimate (see Input Data section) after first satisfying the Ho sink from 1880 to 1976; and the fourth run calculated the NPP variation from 1982 to 1990 required to satisfy the scaled Fr sink estimate (see Input Data section) after first satisfying the Ho sink from 1880 to 1981.

Initial conditions. The initial biomass and soil carbon pool sizes for Experiments 1, 2, and 3 (Table 4) were calculated using an equilibration run, which "spun-up" plant and soil carbon pools using the *Shea* [1986] "mean" climate and calibrated NPP for 1990 for 5000 years (60,000 time steps). After this, another 600-year run was added; each year of this run used a random year of the climate anomaly data [Baker et al., 1995; Hansen and Lebedeff, 1987] from between the years 1880 and 1990 to modulate soil carbon flow.

Experiments 4 and 5 (Table 4) used a different plant and soil carbon initialization since their runs begin in 1880. This initialization is derived from three data sets: (1) monthly precipitation and temperature anomalies from 1880 to 1990 [Baker et al., 1995; Hansen and Lebedeff, 1987]; (2) the historical terrestrial carbon sink estimate of Ho (Figure 2); and (3) NPP derived for experiments 1, 2, and 3, as described above. Using the global, calibrated, annual NPP (57.8 Gt C yr^{-1}) used in Experiment 1, 2, and 3 as a target value for 1990, the initial carbon pool sizes and annual NPP for experiments 4 and 5 were iteratively scaled down such that, following a run with variable climate that scaled NPP each year so that the resulting sink fit the Ho sink estimate, the final global NPP value in 1990 matched the target NPP value. The estimated 1880 global annual NPP rate calculated by this method was 48.1 Gt C yr^{-1}.

Results

Experiment 1:   Carbon turnover dynamics. W e calculated heterotrophic respiration and net carbon exchange under a constant increase in NPP for three cells representing typical grasslands, typical tropical forests, and typical boreal forests (Figure 3). The total equilibrium residence time for each cell τ was determined by dividing the amount of carbon stored in both plants and soils, at equilibrium, by initial annual NPP (P_0). The residence time of the boreal forest cell was 49 years, while the grassland cell's was 10 years and the tropical forest cell's was 21 years. All three cells reached a reasonably stable sink by 150 years, but at different rates. The grassland cell was almost completely stabilized by 40-50 years, while the tropical forest cell required nearly 90 years to do the same. The boreal forest sink was still increasing slightly at 150 years. The time required for each site to reach a stable sink and the sink size both appear to be directly proportional to the turnover time.

Although this is a predictable result from (9), the relative sink size did not match exactly the results of the single-box model. The rate of increase in NPP (0.2% yr^{-1}), as represented by r in (2), and the turnover time of carbon, as represented by k in (4), were held constant, just as assumed by (9), but after 150 years, the numerically modeled sink fell short of the sink expected from (7) by 17.6% for the boreal forest, 26.4% for the grassland, and 7.1% for the tropical forest. An examination of the nature of the carbon pool structure (Figure 1) reveals why: since we use CASA to calculate carbon flow, and there are multiple carbon pools in that model, k, which represents the overall turnover time of the system, no longer represents a single pool but multiple pools. The turnover times of the litter and microbial pools that new carbon first entered were significantly lower than in the soil carbon pools further downstream (Figure 1), so that during the run the effective turnover time of the system dropped while these faster pools increased in size relative to the others, lowering the size of the sink calculated by (7). It should be the case that all locations in which the system is in a positive state of flux will have lower than expected sinks. This, and other aspects of a "front loaded" flow scheme, is what distinguishes CASA from the single-box model in (1)-(10).

Experiment 2:   Global carbon turnover dynamics. At the global scale, with the spatial distribution of residence times and NPP imposed by CASA, and given a spatially uniform r as in (17), the absolute size of the sink should be dependent on both P and τ. Given a constant rate of increase in NPP, the largest sinks should occur in areas with both high NPP and high carbon residence times, as in (9). This is, in
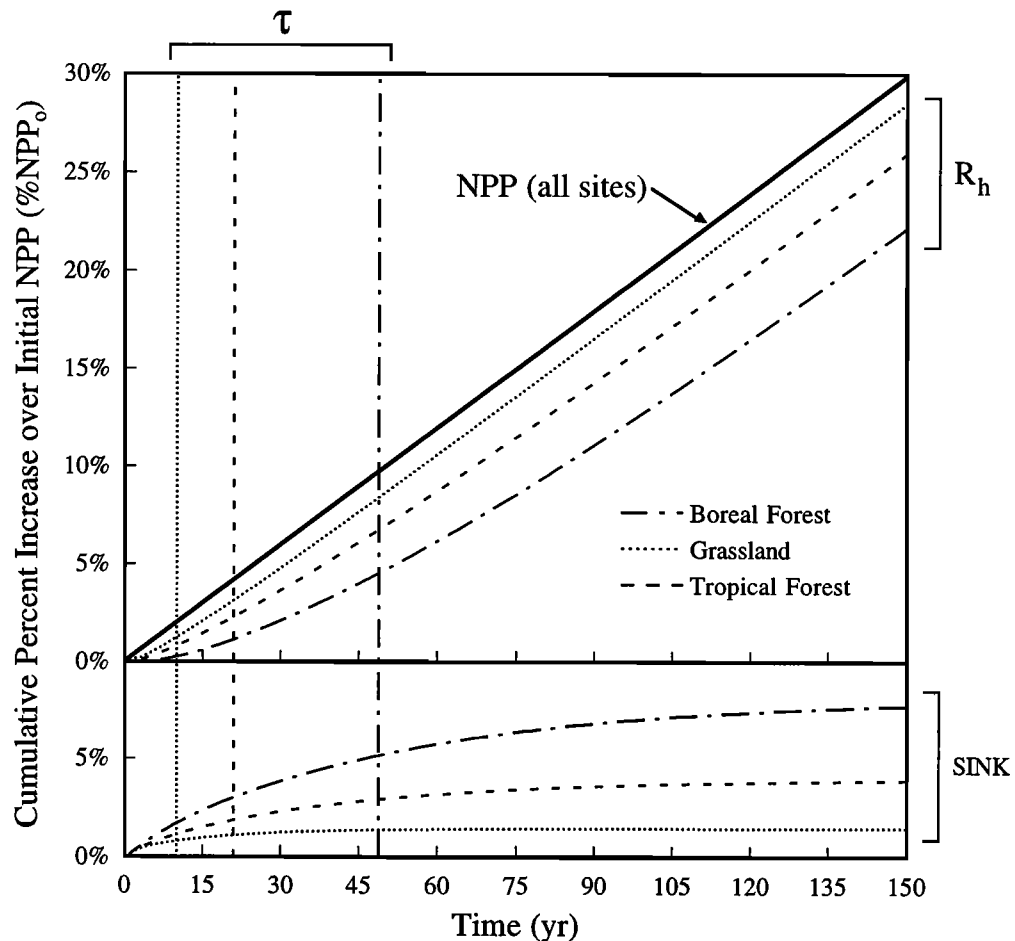
Figure 3. Heterotrophic respiration R_h and the carbon sink following 150 years of 0.2% yr^{-1} increase in annual net primary production (NPP) at three sites (typical grassland cell centered at 41.5° N, 99.5° W, typical tropical forest cell centered at 2.5° S, 59.5° W, and typical boreal forest cell centered at 54.5° N, 66.5° W). The equilibrium turnover time τ of each site is shown as a vertical line intersecting the time axis at τ. NPP, R_h, and the sink of each site are shown relative to the site's initial annual NPP.

fact, what we observed (Plate 2c). The sink was concentrated most strongly in the tropics and secondarily in the northern forests and was almost exclusively due to skew in the spatial distributions of NPP and turnover times (Table 5). The spatial distribution of NPP was strongly biased toward the tropics, where NPP was more than twice as high as anywhere else (Plate 2a), and conversely, the spatial distribution of the equilibrium turnover time of carbon was biased toward northern latitude forests, where τ was almost twice as high as anywhere else (Plate 2b). Areas with low turnover times and low NPP, such as grasslands, tundra, and deserts, did not seem to contribute significantly to the global carbon sink, unlike other regional hot spots aside from boreal and tropical forests, such as the Pacific Northwest of the United States, the eastern United States, southeast Australia and Tasmania, parts of western Europe, central Chile, and northern Argentina, all of which were areas where high NPP and τ coincided.

As in experiment 1, the sink calculated by CASA (Plate 2d) slightly underestimated the sink calculated from (9). When

Table 5. Magnitude and percent of a simulated terrestrial carbon sink found in each vegetation class as defined by *Defries and Townshend* [1994][a]

Vegetation Class	Sink, Tg C / yr	% Global Sink
Broadleaf evergreen trees	737	36.12
Broadleaf deciduous trees	87	4.26
Mixed broadleaf and needleleaf trees	199	9.73
Needleleaf evergreen trees	219	10.74
Needleleaf deciduous trees	82	4.03
Broadleaf trees with ground cover	556	27.26
Perennial grassland	23	1.13
Broadleaf shrubs	20	1.00
Tundra	28	1.36
Hot and cold desert	10	0.48
Agriculture	80	3.91

[a]Numbers based on data from experiment 2, and Plate 2c.
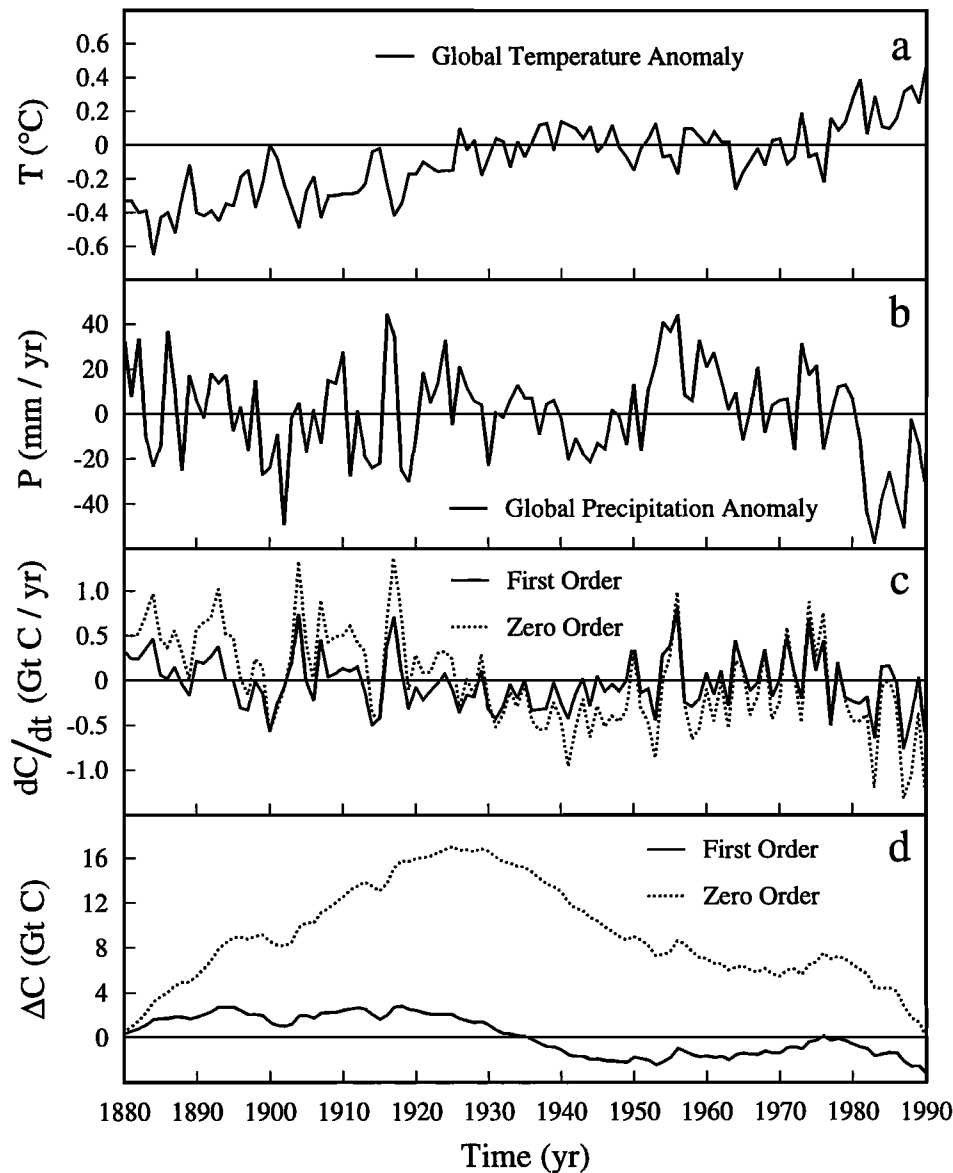
Figure 4. Carbon exchange from 1880 to 1990 for first- and zero-order, climate-driven heterotrophic respiration models under constant NPP conditions, shown against global climate anomalies. (a) The global temperature anomaly [*Hansen and Lebedeff*, 1987] calculated as a land-area weighted average. (b) The global precipitation anomaly [*Baker et al.*, 1995] calculated as a land-area weighted average. (c) Annual carbon exchange due to variation in climate under first-order (climate variation plus carbon pool sizes) and zero-order (climate variation only) heterotrophic respiration models, with annual NPP held constant. Positive values represent a net flux of carbon into the terrestrial biosphere. (d) Cumulative carbon storage (in gigatons C) for the zero-order and first-order models, calculated from Figure 4c. Positive values represent a net storage of carbon in the terrestrial biosphere.

applied to every modeled cell, (9) predicted a 2.25 Gt C yr^{-1} global sink, whereas CASA produced only 2.04 Gt C yr^{-1}. The degree of deviation was greatest in areas with relatively fast turnover in the faster pools (biomass and litter) relative to the slower pools (soil organic matter) (Table 2), in areas where the upper pools decomposed more rapidly due to low litter C:N and low litter lignin (Table 1), or in areas lacking significant woody biomass (such as in grasslands, tundra, or agriculture)

(Table 1). Some additional deviation occurred in regions where climate induced relatively slow decomposition, effectively reducing the amount of time available for the system to react to increases in production, forcing more carbon to stay in faster pools, lowering the effective turnover time of the system, and reducing the magnitude of the sink.

Experiment 3: Climate dependent heterotrophic respiration and carbon exchange over the indus-
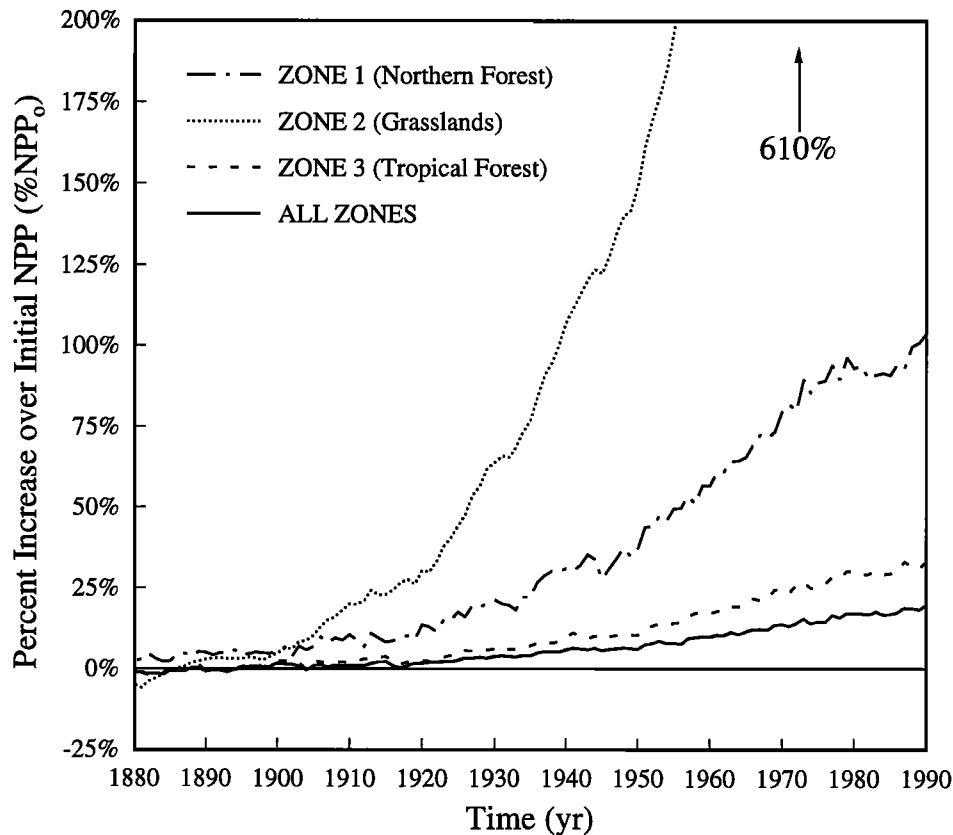
Figure 5. Cumulative change in NPP required to meet the Ho sink estimate when forced into zones 1, 2, 3, and all zones (1, 2, 3, and 4), as shown in Plate 1.

trial period. The first-order model representation in experiment 3 calculated almost no net carbon exchange from 1880 to 1990 (3.2 Gt C release, Figure 4d), and the zero-order model calculated zero net flux, by definition. Global interannual carbon exchange was qualitatively similar but quantitatively divergent under the two models (Figure 4c and 4d). The interannual variability in R_h was greater in the zero-order model by a factor of 2, as was the decadal variability, but the results from the two models were well correlated ($R^2 = 0.74$). Carbon exchange in the first-order model did not exceed far beyond ± 0.5 Gt C yr^{-1}, and the lower rates were due to the additional constraint on carbon flow by negative feedback from changing carbon stocks. It appears that under the first-order model, if anything, R_h increased with time, decreasing the rate of carbon sequestration. The difference in cumulative carbon storage between the models provides an additional illustration of their difference (Figure 4d). The greatest deviation from zero net carbon storage was 16.8 Gt C by the zero-order model and $\pm$ 2.5 Gt C by the first-order model. It is because of the carbon storage feedback that the first-order model was far more constrained than the zero-order model.

Experiment 4: Regional forcing of NPP. Satisfying the Ho sink by increasing NPP in the four zones defined in experiment 4 had different results depending on the biological properties of the zone, its regional climate, and its areal extent (Figure 5). When the sink was forced into all ice-free land area (Plate 1) it was satisfied with a cumulative in-

crease in NPP of the order of 20% by 1990 and not much more than that if the sink was restricted to the tropical forest zone (zone 3). However, if forced into the boreal forest (zone 1), meeting the sink required a 100% cumulative increase in NPP, and if the sink forced into the grassland zone (zone 2), a 610% NPP increase was required.

The β value from (19) for each of these trajectories was of the order of 1.0 and greater. The smallest required b was 0.96 when NPP was forced to satisfy a globally distributed sink (zones 1, 2, 3 and 4), the next largest was 1.57 when the sink was distributed in the tropical zone (zone 3), and following that, β was 4.62 in the boreal zone (zone 1) and 27.5 in the grassland zone (zone 2). The CO_2 sensitivity of NPP implied by this experiment is considerably higher than what is suggested by most studies [*Friedlingstein et al.*, 1995; *Idso et al.*, 1995; *Kimball*, 1983; *Poorter*, 1993; *Schimel*, 1995]. However, if some of the sink is due to factors other than CO_2, then the implied CO_2 sensitivity of NPP should be lower. In addition, turnover times may increase if increased carbon sequestration leads to nitrogen limitation in the soil, thus amplifying changes in NPP with increases in τ.

Because of the relative lack of any gross interannual features in the Ho sink, most of the high frequency variation observed in each of the NPP trajectories is generally attributable to variation in R_h from short-term changes in climate. This is because, in the framework of this study, NPP must not only change to satisfy a prescribed sink estimate but must also in-
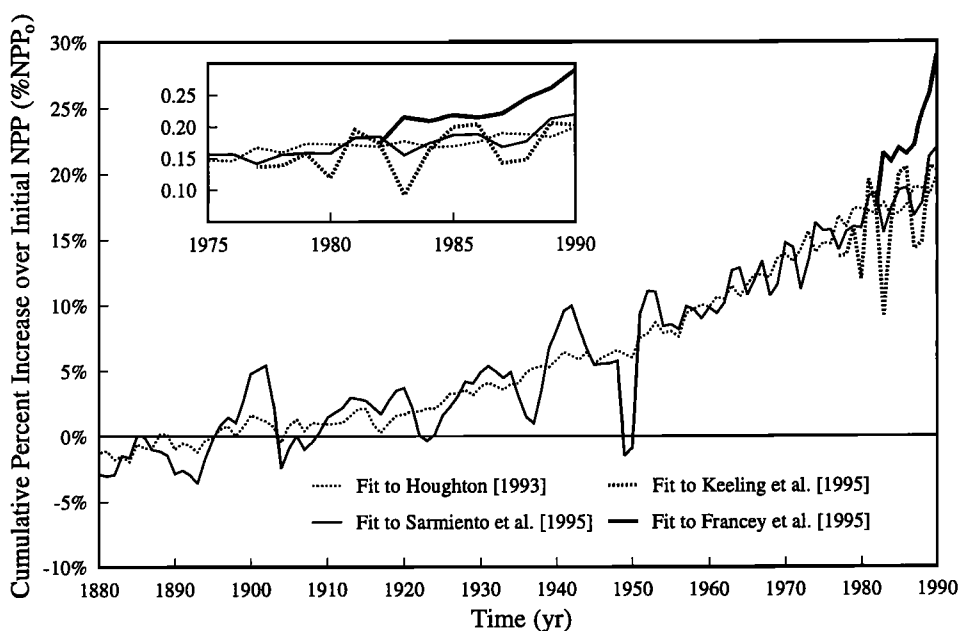
Figure 6. Cumulative percent increase in global NPP required to meet long- and short-term sink estimates (Figure 2), with uniform forcing of NPP for all ice-free land pixels (Plate 1). The same data, from 1975 to 1990, is shown in the inset.

crease or decrease in order to overcome any short-term changes in heterotrophic respiration.

Experiment 5: Global forcing of NPP by different sink estimates. In experiment 5, the cumulative increase in NPP necessary to sustain both the Ho and Sa sinks was about 20%, and on average, a 0.18% annual increase in NPP (0.1 Gt C yr^{-1}) was required to satisfy either long-term sink. The Ke sink estimate imposed the highest average year-to-year variability in NPP ($\pm$ 1.69 Gt C yr^{-1}), while all others imposed considerably lower variation (Fr (1982-1990), $\pm$ 0.79 Gt C yr^{-1}; Sa (1977-1990), $\pm$ 0.64 Gt C yr^{-1} and Ho (1977-1990), $\pm$ 0.31 Gt C yr^{-1}). The variation in NPP imposed by the Ke sink matched closely the variation imposed by the Sa sink (Figure 6), which is not contradictory with the assertion that both sink estimates are derived from roughly the same data (Figure 2). However, clearly a major difference between the two is that the amplitude of variation in the Ke sink is more than twice as high as in the Sa sink during the same period, which is reflected in the fit to the two sink records.

The year-to-year variation in NPP imposed by the Fr sink was qualitatively different from the variation imposed by the other three, as it showed the strongest consistent trend in NPP. This follows largely from the fact that the average sink rate from the Fr estimate is almost twice as high as all the others. Since the carbon pools in that run were initialized by a run from 1880 to 1981 that used the Ho sink estimate, the sharp break in the rate of the sink in 1982 caused a correspondingly sharp increase in the required rate of increase in NPP, as would be expected from (9). The interannual variation in the short-term variation in the fit to the Fr sink, however, did not agree so closely with fits to the other sinks, and the fit to the Ho data was interannually relatively featureless.

Discussion

Dynamics of carbon cycling in the terrestrial biosphere. By definition, at equilibrium, the annual rate of heterotrophic respiration equals the rate of input of carbon into the heterotrophic community. If heterotrophic respiration is a first-order process, then it will increase as carbon storage increases, and carbon storage will increase as NPP increases. Thus the rate of change in respiration is linked to change in NPP, but because of the time delay between change in the two processes, the link operates primarily on timescales of decades.

From experiment 1 (Figure 3), it is clear that the relative size and formation time of the sink following a perturbation in NPP is largely dependent on the turnover time of carbon in the system. The longer the time delay between the sequestration of carbon and its release determines how far NPP can exceed R_h, and how quickly. However, there are other factors that affect the ultimate size of the sink (experiment 2, Plate 2d). Globally, regions with fast carbon turnover rates in plants and at the surface, where carbon is first deposited, have lower integrated turnover times as long as new carbon is being introduced (Table 1), which effectively lowers the potential sink. Conversely, regions with finely textured soils (Table 2) will also have lower integrated turnover times, since the disparity between the turnover times in soil organic matter relative to the turnover times in plants and litter will be widened whenever the turnover times of soil organic matter decline. It is very important, when calculating the integrated turnover time of a system in flux, that the full dynamics of all the pools, as well as the location and magnitude of the inputs, are taken into account.

NPP and respiration are decoupled slightly by changes in climate and its effect on respiration (experiment 3). However, on timescales of decades, following climate perturbations resulting in significant loss or gain of carbon, and barring significant changes in NPP, ecosystems should eventually return to a steady state as carbon stocks and soil respiration equilibrate with the new climate and NPP (Figure 4). Under CASA (experiment 3), the climate variation observed over the last 110 years resulted in a net loss of carbon of only 1.8 Gt C for the entire period, almost 2 orders of magnitude smaller than the cumulative net exchange estimated by either of the long-term sink estimates (Figure 2). In addition, even under the more variable of the two models, ΔC (< 17 Gt C, Figure 4d) did not approach the cumulative carbon sequestration estimated by the two long-term estimates (~93 Gt C, see Input Data section), suggesting that, on timescales of decades, R_h is a weak force in determining carbon exchange and that the force overwhelmingly responsible for the sink estimated by either Ho or Sa is change in NPP. It should be noted, however, that this model restricts itself to change in NPP and R_h to explain changes in carbon storage. There is considerable evidence that, in the last century, a large part of the sink could be attributable to temperate, boreal, and tropical forest regrowth [Houghton, 1995].

If NPP were to stop increasing for any reason, the carbon sink would decline to zero flux in a matter of years to decades. This is an important point; the size of the carbon sink is dependent on the rate at which NPP is increasing:

$$\frac{dC(t)}{dt} \propto r \qquad (20)$$

not on the cumulative increase in NPP over the industrial period:

$$\frac{dC(t)}{dt} \propto \int r \, dt \quad \text{not true.} \qquad (21)$$

The rate of increase in NPP can change in one of two general ways: (1) a decline in the rate of growth of stimulating factors (such as climate or CO_2 and nitrogen fertilization) or (2) an acclimation of plants to stimulating factors.

Location of the carbon sink under a globally uniform increase in NPP. As asserted in (9), the size of the sink over a period of time is proportional to NPP, the turnover time of carbon and the rate at which NPP is increasing. The iteratively calculated sink in experiment 2 is consistent with (9), in that it is distributed primarily in the tropics (classes 1 and 6), and secondarily in the northern softwood and hardwood forests (classes 3 and 4), where both NPP and τ are relatively high. Others have estimated sink distributions similar to this from the perspective of atmospheric data and tracer transport models [Ciais et al., 1995] and mechanistic models [Friedlingstein et al., 1995].

There are a number of important points to make from this. First, the potential sink is conspicuously low in a number of regions (Plate 2c). The world's grassland, tundra, and desert regions do not appear to have the capacity to sequester carbon at a rate approaching that of the boreal forests, let alone the tropics, and it seems unlikely from this study that grasslands should be major sinks (Figures 3 and 5). Some studies highlight the potential for carbon storage in grasslands [Parton et

al., 1995; Thornley et al., 1991], but the biogeochemical constraints on the sink, as defined in this study, make a sink in this biome difficult without a large rate of increase in NPP (Figures 3 and 5). Second, areas with the highest potential response to increasing CO_2 [Mooney et al., 1991], or nitrogen fertilization, are not necessarily those places that, given the same relative increase in NPP, would have the highest biogeochemical potential for a sink. For example, grasslands probably have a fairly high potential response curve to increases in CO_2, but the resultant rate of increase in NPP is unlikely to maintain a substantial sink when juxtaposed with initially low NPP and a relatively high rate of carbon turnover. And third, under the assumptions of this study, the potential sink is most likely to be strongest in the boreal and tropical forests. The combination of high wood turnover times, slow soil organic matter turnover (in cold regions), and high NPP give these biomes the greatest potential for carbon storage.

Historical variation in net primary production. In experiment 4, the relative change in NPP varied considerably, depending on the biogeochemical potential of the region into which the Ho sink was forced. Of all the runs in experiment 4, the smallest cumulative increase in NPP was required when regionally unconstrained (i.e., allowed to occupy all ice-free land area in Plate 1). As stated before, this increase required a β of 0.96, which is fairly large in the context of the β values calculated by other studies.

The higher rates of NPP increase required to satisfy the sink when forced into each of zones 1, 2, and 3 (Plate 1) show how a reduction in areal extent, and a general decrease in the sink potential of a region due to a combination of lower NPP and turnover times, can affect the required response in NPP. The sensitivity of this study to the initial distribution of NPP and τ opens this to a number of different interpretations. For instance, we found that by increasing the global magnitude of the target NPP in 1990 (see Model Experiments section) from 57.8 Gt C yr^{-1} to 70 Gt C yr^{-1}, recalculating initial NPP and carbon storage in 1880, and rerunning experiment 4 based on this new constraint, the cumulative increase in NPP required to satisfy the Ho sink dropped from 20% to 14%, and β dropped from 0.96 to ~0.65. In addition, if we changed the distribution of NPP and τ, such that the turnover time of carbon and the magnitude of NPP in the boreal forest were higher, this region accounted for a larger portion of the resulting sink, necessitating a smaller increase in NPP.

The required variation in NPP is also sensitive to the size of the sink estimate employed as a constraint. If the sink increases while initial NPP remains constant, to balance (8), the rate of increase in NPP must also increase. An example of this can be found in experiment 5 when the Fr sink estimate is used. This sink estimate, which is on average twice as high as the others, required a rate of increase in NPP that was dramatically higher than the others. In addition, if the sink estimate were to drop to zero in magnitude, the required increase in NPP would also drop to zero.

The results of experiment 5 (Figure 6) show that, over timescales of decades and longer, any sink estimate that has nearly the same magnitude as another will require about the same long-term change in NPP to satisfy it. In addition, the large variability in the sink from year-to-year (1977-1990) in most of the estimates was clearly observed in the NPP trajecto-

ries (Figure 6, inset), especially in the Ke estimate. It is not clear whether the strong variation in NPP required by these sink estimates is reasonable, since there have been no direct observations of global NPP on interannual timescales.

What is clear, however, is that a consistent increase in NPP is required to sustain a constant sink rate. Heterotrophic respiration is controlled to a large extent by changes in climate, but the cumulative, climate-induced change in carbon storage is not on the same order of magnitude as that of the sink over long time scales. In addition, since heterotrophic respiration will continuously approach a balance with inputs of new carbon, the rate of respiration will be set largely by change in NPP, leaving change in NPP to account for the greater portion of the sink.

Conclusions

1. The carbon sink can be roughly calculated as the product of annual net primary production, the annual relative rate of increase in NPP, and the turnover time of carbon in the system. This means that, given a consistent rate of increase in NPP among sites, the regions with the highest potential carbon sink will be those with high NPP and slow carbon turnover, such as tropical and boreal forests. CASA provides a close approximation to this rule, but the greatest deviations in CASA from that rule occur in regions where the system is sensitive to "front loading" that occurs when there is a flux of carbon into the biosphere.

2. Long-term climatic change may not be the most important direct controller of global heterotrophic respiration. Only a small change in heterotrophic respiration over the period of this study can be attributed solely to changes in climate. The first-order nature of the heterotrophic community and the negative feedback that exists whenever carbon stocks increase or decrease make this so. Since climate does not seem to significantly decouple NPP and respiration, NPP, which may in fact be strongly influenced by changes in climate, appears to be the primary factor determining the rate of heterotrophic respiration.

3. The maintenance of a terrestrial carbon sink over extended periods of time requires a small, but consistent, increase in NPP. From 1880 to 1990, the change in R_h due to climate variation does not approach the rate of carbon exchange prescribed by the Ho and Sa sink estimates. Thus we predict that net carbon exchange will depend mostly on the rate of change in NPP.

4. If NPP were to stop increasing in a region where there is a net carbon sink, the sink will eventually disappear. The size of carbon sink depends not on how much stimulation is occurring but on the rate of increase in stimulation.

References

Baker, C. B., J. K. Eischeid, T. R. Karl, and H. F. Diaz, The quality control of long-term climatological data using objective data analysis, in *Preprints of AMS Ninth Conference on Applied Climatology*, Natl. Climatic Data Cent., Asheville, N.C., 1995.

Bishop, J. K. B., and W. B. Rossow, Spatial and temporal variability of global surface solar irradiance, *J. Geophys. Res.*, 96, 16,839-16,858, 1991.

Ciais, P., P. P. Tans, M. Trolier, J. W. C. White, and R. J. Francey, A large northern hemispheric CO$_2$ sink indicated by the ^{13}C/^{12}C ratio of atmospheric CO$_2$, *Science*, 269, 1098-1102, 1995.

Conway, T. J., P. P. Tans, L. S. Waterman, K. W. Thoning, D. R. Kitzis, K. A. Masarie, and N. Zhang, Evidence for interannual variability of the carbon cycle from the National Oceanic and Atmospheric Administration/Climate Monitoring and Diagnostics Laboratory Global Air Sampling Network, *J. Geophys. Res.*, 99, 22,831-22,855, 1994.

Dai, A., and I. Y. Fung, Can climate variability contribute to the "missing" CO$_2$ sink?, *Global Biogeochem. Cycles*, 7, 599-609, 1993.

Defries, R. S., and J. R. G. Townshend, NDVI-derived land cover classification at a global scale, *Int. J. Remote Sens.*, 15, 3567-3586, 1994.

Enting, I. G., A synthesis inversion of the concentration and δ^{13}C of atmospheric CO$_2$, *Tellus Ser. B*, 47, 35-52, 1995.

Enting, I. G., and J. V. Mansbridge, Latitudinal distribution of sources and sinks of CO$_2$: results of an inversion study, *Tellus Ser. B*, 43, 156-170, 1991.

Field, C. B., J. T. Randerson, and C. M. Malmström, Global net primary production: combining ecology and remote sensing, *Remote Sens. Environ.*, 51, 74-88, 1995.

Francey, R. J., P. P. Tans, C. E. Allison, I. G. Enting, J. W. C. White, and M. Trolier, Changes in oceanic and terrestrial carbon uptake since 1982, *Nature*, 373, 326-330, 1995.

Friedli, H., H. Lötscher, H. Oeschger, U. Siegenthaler, and B. Stauffer, Ice core record of the ^{13}C/^{12}C ratio of atmospheric CO$_2$ in the past two centuries, *Nature*, 324, 237-238, 1986.

Friedlingstein, P., I. Fung, E. Holland, J. John, G. Brasseur, D. Erickson, and D. Schimel, On the contribution of CO$_2$ fertilization to the missing biospheric sink, *Global Biogeochem. Cycles*, 9, 541-556, 1995.

Fung, I. Y., K. Prentice, E. Matthews, J. Lerner, and G. Russell, Three dimensional tracer model study of atmospheric CO$_2$: response to seasonal exchanges with the terrestrial biosphere, *J. Geophys. Res.*, 88, 1281-1294, 1983.

Gifford, R. M., The global carbon cycle: A viewpoint on the missing sink, *Aust. J. Plant Physiol.*, 21, 1-15, 1994.

Grace, J., J. Lloyd, J. McIntyre, A. Miranda, P. Meir, H. Miranda, J. Moncrieff, J. Massheder, I. Wright, and J. Gash, Fluxes of carbon dioxide and water vapour over an undisturbed tropical forest in south-west Amazonia, *Global Change Biol.*, 1, 1-12, 1995.

Hansen, J., and S. Lebedeff, Global trends of measured surface air temperature, *J. Geophys. Res.*, 92, 13,345-13,372, 1987.

Hansen, J., and S. Lebedeff, Global surface air temperatures: Update through 1987, *Geophys. Res. Lett.*, 15, 323-326, 1988.

Heimann, M., C. D. Keeling, and C. J. Tucker, A three-dimensional model of atmospheric CO$_2$ transport based on observed winds, 3, Seasonal cycle and synoptic timescale variations, in *Aspects of Climatic Variability in the Pacific and the Western Americas, Geophys. Monogr. Ser.*, vol. 55, edited by D. H. Peterson, pp. 277-303, Washington, D. C., 1989.

Holland, E. A., A. R. Townsend, and P. M. Vitousek, Variability in temperature regulation of CO$_2$ fluxes and N mineralization from five Hawaiian soils: Implications for a changing climate, *Global Change Biol.*, 1, 115-123, 1995.

Houghton, R. A., Biotic changes consistent with the increased seasonal amplitude of atmospheric CO$_2$ concentrations, *J. Geophys. Res.*, 92, 4223-4230, 1987.

Houghton, R. A., Changes in terrestrial carbon over the last 135 years, in *The Global Carbon Cycle*, edited by M. Heimann, pp. 139-157, Springer-Verlag, New York, 1993.

Houghton, R. A., Land-use change and the carbon cycle, *Global Change Biol.*, 1, 275-287, 1995.

Hudson, R. J. M., S. A. Gherini, and R. A. Goldstein, Modeling the global carbon cycle: Nitrogen fertilization of the terrestrial biosphere and

the "missing" CO_2 sink, *Global Biogeochem. Cycles, 8*, 307-333, 1994.

Idso, S. B., K. E. Idso, R. L. Garcia, B. A. Kimball, and J. K. Hoober, Effects of atmospheric CO_2 enrichment and foliar methanol application on net photosynthesis of sour orange tree (*Citrus aurantium*: Rutaceae) leaves, *Am. J. Bot., 82*, 26-30, 1995.

Keeling, C. D., and T. P. Whorf, Atmospheric CO_2 records from sites in the SIO air sampling network, in *Trends '93: A Compendium of Data on Global Change*, edited by T. A. Boden, D. P. Kaiser, R. J. Sepanski, and F. W. Stoss, *Rep. ORNL/CDIAC-65*, pp. 16-26, Carbon Dioxide Inf. Anal. Cent., Oak Ridge Natl. Lab., Oak Ridge, Tenn., 1994.

Keeling, C. D., T. P. Whorf, M. Wahlen, and J. van der Plicht, Interannual extremes in the rate of rise of atmospheric carbon dioxide since 1980, *Nature, 375*, 666-670, 1995.

Kimball, B. A., Carbon dioxide and agricultural yield: An assemblage and analysis of 430 prior observations, *Agron. J., 75*, 779-788, 1983.

Kohlmaier, G. H., et al., The Frankfurt Biosphere Model: a global process-oriented model for the seasonal and long term CO_2 exchange between terrestrial ecosystems and the atmosphere: Global results, *Climate Research*, in press.

Lieth, H., Modeling the primary productivity of the world, in *Primary Productivity of the Biosphere*, edited by H. Lieth, and R. H. Whittaker, pp. 237-263, Springer-Verlag, New York, 1975.

Lloyd, J., and J. A. Taylor, On the temperature dependence of soil respiration, *Funct. Ecol., 8*, 315-323, 1994.

Los, S. O., C. O. Justice, and C. J. Tucker, A global 1° by 1° NDVI data set for climate studies derived from the GIMMS continental NDVI data., *Int. J. Remote Sens., 15*, 3493-3518, 1994.

Maisongrande, P., A. Ruimy, G. Dedieu, and B. Saugier, Monitoring seasonal and interannual variations of gross primary productivity, net primary productivity and net ecosystem productivity using a diagnostic model and remotely-sensed data, *Tellus Ser. B, 47*, 178-190, 1995.

Marland, G., and R. M. Rotty, Carbon dioxide emissions from fossil fuels: A procedure for estimations and results for 1950-1982, *Tellus Ser. B, 36*, 232-261, 1984.

Melillo, J. M., D. W. Kicklighter, A. D. McGuire, B. Moore III, C. J. Vorosmarty, and A. L. Grace, Global climate change and terrestrial net primary production, *Nature, 363*, 234-240, 1993.

Mooney, H. A., B. G. Drake, R. J. Luxmoore, W. C. Oechel, and L. F. Pitelka, Predicting ecosystem responses to elevated CO_2 concentrations, *BioScience, 41*, 96-104, 1991.

Moore, B., III, and B. H. Braswell, The lifetime of excess atmospheric carbon dioxide, *Global Biogeochem. Cycles, 8*, 23-38, 1994.

Neftel, A., H. Oeschger, J. Schwander, B. Stauffer, and R. Zumbrunn, Ice core measurements give atmospheric pCO_2 content during the past 40,000 years, *Nature, 295*, 220-223, 1982.

Neftel, A., H. Friedli, E. Moor, H. Oeschger, U. Siegenthaler, and B. Stauffer, Historical CO_2 record from the Siple Station ice core, in *Trends '93: A Compendium of Data on Global Change*, edited by T. A. Boden, D. P. Kaiser, R. J. Sepanski, and F. W. Stoss, *Rep. ORNL/CDIAC-65*, pp. 11-14, Carbon Dioxide Inf. Anal. Cent., Oak Ridge Natl. Lab., Oak Ridge, Tenn., 1994.

Parton, W. J., et al., Observations and modeling of biomass and soil organic matter dynamics for the grassland biome worldwide, *Global Biogeochem. Cycles, 7*, 785-809, 1993.

Parton, W. J., J. M. O. Scurlock, D. S. Ojima, D. S. Schimel, D. O. Hall, and S. G. Members, Impact of climate change on grassland production and soil carbon worldwide, *Global Change Biol., 1*, 13-22, 1995.

Poorter, H., Interspecific variation in the growth response of plants to an elevated ambient CO_2 concentration, *Vegetatio, 104/105*, 77-97, 1993.

Post, W. M., W. R. Emanuel, P. J. Zinke, and A. G. Stangenberger, Soil carbon pools and world life zones, *Nature, 298*, 156-159, 1982.

Potter, C. S., J. T. Randerson, C. B. Field, P. A. Matson, P. M. Vitousek, H. A. Mooney, and S. A. Klooster, Terrestrial ecosystem production: A process model based on global satellite and surface data, *Global Biogeochem. Cycles, 7*, 811-841, 1993.

Raich, J. W., and C. S. Potter, Global patterns of carbon dioxide emissions from soils, *Global Biogeochem. Cycles, 9*, 23-36, 1995.

Randerson, J. T., M. V. Thompson, C. M. Malmström, C. B. Field, and I. Y. Fung, Substrate limitations for heterotrophs: Implications for models that estimate the seasonal cycles of atmospheric CO_2, *Global Biogeochem. Cycles*, in press, 1996.

Sarmiento, J. L., C. Le Quéré, and S. W. Pacala, Limiting future atmospheric carbon dioxide, *Global Biogeochem. Cycles, 9*, 121-137, 1995.

Schimel, D. S., Terrestrial ecosystems and the carbon cycle, *Global Change Biol., 1*, 77-91, 1995.

Schimel, D. S., I. Enting, M. Heimann, T. M. L. Wigley, D. Raynaud, D. Alves, and U. Siegenthaler, CO_2 and the carbon cycle, in *IPCC WGI Report: Radiative Forcing of Climate Change*, edited by J. T. Houghton, and L. G. Meira Filho, 572 pp. Cambridge Univ. Press, New York, 1995.

Schindler, D. W., and S. E. Bayley, The biosphere as an increasing sink for atmospheric carbon: Estimates from increased nitrogen deposition, *Global Biogeochem. Cycles, 7*, 717-733, 1993.

Sellers, P. J., C. J. Tucker, G. J. Collatz, S. O. Los, C. O. Justice, D. A. Dazlich, and D. A. Randall, A global 1° by 1° NDVI data set for climate studies, 2, The generation of global fields of terrestrial biophysical parameters from the NDVI., *Int. J. Remote Sens., 15*, 3519-3545, 1994.

Shea, D. J., Climatological atlas: 1950-1979, *Tech. Note NCAR TN-269+STR*, Natl. Cent. for Atmos. Res., Boulder, Colo., 1986.

Siegenthaler, U., and J. L. Sarmiento, Atmospheric carbon dioxide and the ocean, *Nature, 365*, 119-125, 1993.

Siegenthaler, U., H. Friedli, H. Lötscher, E. Moor, A. Neftel, H. Oeschger, and B. Stauffer, Stable-isotope ratios and concentration of CO_2 in air from polar ice cores, *Ann. Glaciol., 10*, 1-6, 1988.

Tans, P. P., I. Y. Fung, and T. Takahashi, Observational constraints on the global atmospheric CO_2 budget, *Science, 247*, 1431-1438, 1990.

Thornley, J. H. M., D. Fowler, and M. G. R. Cannell, Terrestrial carbon storage resulting from CO_2 and nitrogen fertilization in temperate grasslands, *Plant Cell Environ., 14*, 1007-1011, 1991.

Vorosmarty, C. J., B. Moore III, A. L. Grace, M. P. Gildea, J. M. Melillo, B. J. Peterson, E. B. Rastetter, and P. A. Steudler, Continental scale models of water balance and fluvial transport: an application to South America, *Global Biogeochem. Cycles, 3*, 241-265, 1989.

Zobler, L. A., World soil file for global climate modeling, *NASA Tech. Memo. 87802*, 32 pp., 1986.

C. B. Field, C. M. Malmström, and J. T. Randerson, Department of Plant Biology, Carnegie Institution of Washington, 290 Panama Street, Stanford, CA 94305-1297. (e-mail: chris@jasper.stanford.edu; carolyn@jasper.stanford.edu; orcinus@jasper.stanford.edu)

M. V. Thompson, Department of Organismic and Evolutionary Biology, Harvard University, 16 Divinity Avenue, Cambridge, MA 02138. (e-mail: mthompso@oeb.harvard.edu)